Available online at www.sciencedirect.com
ScienceDirect
Chinese Journal of Natural Medicines 2023, **21**(6): 443-453
doi: 10.1016/S1875-5364(23)60472-8
Chinese Journal of Natural Medicines

•Original article•

Bioassay-guided isolation of α-Glucosidase inhibitory constituents from *Hypericum sampsonii*

TAO Linlan[1, 2, 3Δ], XU Shuangyu[1, 2, 3Δ], ZHANG Zizhen[1, 2, 3], LI Yanan[1, 2, 3], YANG Jue[1, 2, 3], GU Wei[1, 2, 3], YI Ping[1, 2, 3*], HAO Xiaojiang[1, 2, 3, 4*], YUAN Chunmao[1, 2, 3*]

[1] *State Key Laboratory of Functions and Applications of Medicinal Plants, Guizhou Medical University, Guiyang 550014, China;*
[2] *School of Pharmaceutical Sciences, Guizhou Medical University, Guiyang 550025, China;*
[3] *Natural Products Research Center of Guizhou Province, Guiyang 550014, China;*
[4] *State Key Laboratory of Phytochemistry and Plant Resources in West China, Kunming Institute of Botany, Chinese Academy of Sciences, Kunming 650201, China*

Available online 20 Jun., 2023

[ABSTRACT] This study employed the α-glucosidase inhibitory activity model as an anti-diabetic assay and implemented a bioactivity-guided isolation strategy to identify novel natural compounds with potential therapeutic properties. *Hypericum sampsonii* was investigated, leading to the isolation of two highly modified seco-polycyclic polyprenylated acylphloroglucinols (PPAPs) (**1** and **2**), eight phenolic derivatives (**3**–**10**), and four terpene derivatives (**11**–**14**). The structures of compounds **1** and **2**, featuring an unprecedented octahydro-2H-chromen-2-one ring system, were fully characterized using extensive spectroscopic data and quantum chemistry calculations. Six compounds (**1**, **5**–**7**, **9**, and **14**) exhibited potential inhibitory effects against α-glucosidase, with IC_{50} values ranging from 0.050 ± 0.0016 to 366.70 ± 11.08 μg·mL^{-1}. Notably, compound **5** (0.050 ± 0.0016 μg·mL^{-1}) was identified as the most potential α-glucosidase inhibitor, with an inhibitory effect about 6900 times stronger than the positive control, acarbose (IC_{50} = 346.63 ± 15.65 μg·mL^{-1}). A docking study was conducted to predict molecular interactions between two compounds (**1** and **5**) and α-glucosidase, and the hypothetical biosynthetic pathways of the two unprecedented seco-PPAPs were proposed.

[KEY WORDS] *Hypericum sampsonii*; Chemical constituents; Structure elucidation; α-Glucosidase; Molecular docking
[CLC Number] R284.1 **[Document code]** A **[Article ID]** 2095-6975(2023)06-0443-11

Introduction

Diabetes mellitus (DM) is a chronic metabolic disorder that is characterized by persistent hyperglycemia due to insulin resistance, relative insulin insufficiency, and increased endogenous glucose production [1]. According to the International Diabetes Federation report, the number of adults (20–79 years) with DM is currently 537 million and is projected to rise to over 642 million in 2040 [2]. Glycemic control is a cornerstone of the long-term treatment of DM [3]. Targeting key enzymes involved in the pathogenesis of DM is a pivotal strategy for controlling hyperglycemia. While several drugs that inhibit these key enzymes, such as acarbose, sitagliptin phosphate, and rosiglitazone, are available, they are associated with numerous adverse effects. Therefore, the discovery of new anti-diabetic drugs with minimal or no side effects has become a critical research area.

To date, numerous therapeutic targets have been identified for the anti-diabetic drugs. Among these, two well-established targets for reducing postprandial hyperglycemia induced by starch digestion in the small intestine α-glucosidase and α-amylase are two well-validated therapeutic targets [4]. Moreover, protein tyrosine phosphatase 1B (PTP1B) has emerged as a novel and promising therapeutic target for treating type II DM, as it negatively regulates the signaling path-

[Received on] 12-Oct.-2022
[Research funding] The work was supported by the National Natural Science Foundation of China (No. 32270413, U1812403), the Science and Technology Department of Guizhou Province (No. QKH 2020-1Z076), the 13th batch of Outstanding Young Scientific and Technological Talents in Guizhou Province (No. QKHPTRC [2021]5633), Cultivation project of National Natural Science Foundation of Guizhou Medical University (No. 19NSP003), the Education Department of Guizhou Province (No. QJH KY [2021]189), the Natural Science Foundation of Guizhou Province (No. QKHZYD[2022]4015), High-level Innovative Talents in Guizhou Province (Thousand Levels of Talent for Chunmao Yuan in 2018), and "Light of the West" Talent Cultivation Program of Chinese Academy of Sciences for Chunmao Yuan (No. RZ [2020]82).
[*Corresponding author] E-mails: yiping2100@aliyun.com (YI Ping); haoxj@mail.kib.ac.cn (HAO Xiaojiang); yuanchunmao01@126.com (YUAN Chunmao)
[Δ]These authors contributed equally to this work.
These authors have no conflict of interest to declare.

ways of leptin and insulin receptors [5-6]. Thus, the search for new inhibitors on the above-mentioned proteins is a pivotal strategy for the discovery and development of effective anti-diabetic drugs with minimal adverse effects.

Hypericum sampsonii, a perennial herb, is widely distributed in southern China, north Vietnam, and eastern Burma [7]. This palnt, known as "Yuan Baocao" in Traditional Chinese Medicine, has been utilized in treating various ailments, including backache, burns, diarrhea, snakebites, and swelling [8]. Previous phytochemical investigations have shown that this plant is rich in flavonoids, xanthones, benzophenones, anthraquinones, and polycyclic polyprenylated acylphloroglucinols (PPAPs) [9-10]. These compounds exhibited a wide range of bioactivities, such as anti-tumor, anti-viral, anti-bacterial, anti-oxidative, multi-drug resistance reversal, and anti-inflammatory activities [11-12]. However, there has been no comprehensive study on the anti-diabetic properties of *H. sampsonii*. Thus, this study employed the α-glucosidase inhibitory activity model as an anti-diabetic assay and implemented a bioactivity-guided isolation strategy to identify novel natural compounds with potential therapeutic properties.

Results and Discussion

The present study evaluated the inhibitory effects of ethyl acetate (EA) and water (WT) fractions derived from *H. sampsonii* against α -glucosidase (Fig. 1). The results revealed that the EA fraction could significantly inhibit α-glucosidase, with an inhibitory ratio of 64% at the concentration of 100 μg·mL^{-1}, while the WT fraction displayed no inhibitory activity at the same concentration. Therefore, the EA fraction was further analyzed for its IC_{50} value, which was determined to be 54.86 μg·mL^{-1}. Notably, this value was six times higher than that observed for the positive control, acarbose (346.60 μg·mL^{-1}).

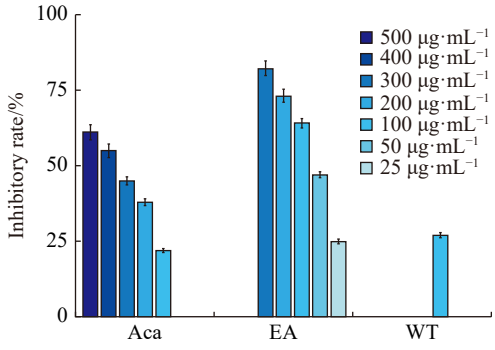

Fig. 1 α-Glucosidase inhibitory rate for extracts in different concentration. Aca: acarbose, the positive control. EA: ethyl acetate extracts. WT: water extracts.

Further isolation of the active EA fraction yielded a total of 14 compounds, including two novel seco-PPAPs (**1** and **2**), four terpene derivatives (**11**–**14**), and eight phenolic derivatives (**3**–**10**). Twelve of these compounds, namely l-hydroxy-7-methoxyxanthone (**3**) [13], 4-hydroxyxanthone (**4**) [14], 1,3,6,7-tetrahydroxyxanthone (**5**) [15], dihydroquercetin (**6**) [16], quercetin (**7**) [17], 4-geranyloxy-2,6-dihydroxybenzophenone (**8**) [18], methyl 3-oxo-3-phenyl propanoate (**9**) [19], norhypersampsone A (**10**) [20], hyperpyran A (**11**) [21], betulinic acid (**12**) [22], α-tocospiro A (**13**) [23], and trans-phytol (**14**) [24] (Fig. 2), were identified as known compounds based on a comprehensive comparison of NMR and MS spectroscopic data with literature references.

Hypsampsonione A (**1**) was isolated as a colorless oil. Its molecular formula was established as $C_{38}H_{50}O_5$ by high-resolution electrospray ionization mass spectrometry (HR-ESI-MS) at *m/z* 587.3728 $[M + H]^+$ (Calcd. for $C_{38}H_{51}O_5$: 587.3731), with 14 degrees of unsaturation. Analysis of the ^{1}H nuclear magnetic resonance (NMR) spectrum of **1** (Tab. 1) showed the characteristic signals of a phenyl group (δ_H 7.88, 2H, d, J = 7.5 Hz; 7.66, 1H, t, J = 7.5 Hz; 7.54, 2H, t, J = 7.5 Hz), three olefinic protons (δ_H 5.16, 1H, t, J = 7.1 Hz; 5.12, 1H, t, J = 7.9 Hz; 5.08, 1H, t, J = 7.5 Hz), and nine methyl groups (δ_H 1.71, s; 1.62, s; 1.61, s; 1.59, s; 1.53, s; 1.16, s; 1.10, s; 0.99, s; 0.96, s). The ^{13}C NMR (Tab. 1) and HSQC spectra confirmed the presence of 38 carbons in **1**, including nine methyls, six methylenes, ten methines (eight olefinic carbons), and thirteen quaternary carbons (two carbonyls and seven olefinic carbons). The spectra also revealed that **1** contained a three-ring system in addition to a phenyl group, two carbonyls, and five double bonds, accounting for a total of 11 degrees of unsaturation.

From the ^{1}H–^{1}H COSY cross-peaks in Fig. 3, five fragments (**a**–**e**) were assigned based on their highlighted bonds. Using the heteronuclear multiple bond correlation (HMBC) spectrum, the linkages of these four fragments established. HMBC correlations from Me-30 to C-27, C-28, and C-29, from Me-34 to C-32, C-33, and C-35, and from Me-24 to C-22, C-23, and C-25 revealed the presence of an isopentenyl and a geranyl group. The connections of C-1, Me-20, and C-3 (fraction **a**) to C-2 were established by HMBC correlations from Me-20 to C-1, C-2, and C-3. Moreover, fragments **a** and **b**, C-11, and C-6 were connected to each other through C-5, as confirmed by HMBC correlations from H_2-26 to C-4, C-5, C-6, and C-11. The HMBC correlations from OH-36 to C-7, C-36, and C-38, and from Me-37 to C-36 and C-7 indicated that 2-hydroxypropan-2-yl was linked to fragment **d**. The furan ring (ring A) was established from vital HMBC correlations from H_2-8 to C-6 and C-9, along with a characteristic oxidized CH (δ_C 93.0) and a typical oxidized olefinic carbon (δ_C 176.5), which were in good agreement with those in a previous study [25]. However, another two-ring system (rings B and C) and the location of a benzoyl group could not be confirmed due to the lack of key 2D NMR data.

Computer-assisted structure elucidation (CASE) is a widely accepted approach used to overcome challenges associated with the analysis of new natural products [26-27]. In the present study, CASE was employed to determine the structure of compound **1** by inputting the experimental 1D and 2D NMR data, along with its molecular formula, into the ACD/Structure Elucidator Suite. After adjusting general para-

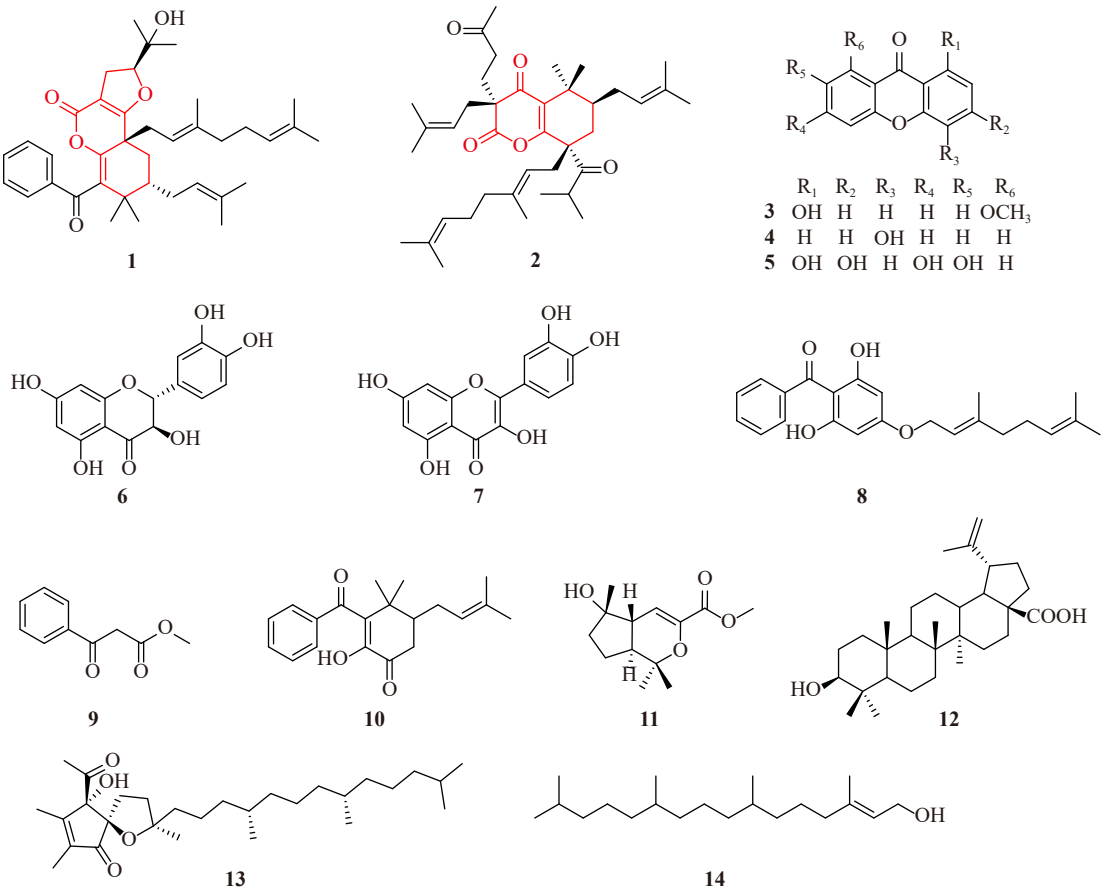

Fig. 2 Compounds isolated from *H. sampsonii*.

meters, 100 possible structures were generated and filtrated (Supporting Information). The structure with the highest R^2 and lowest standard deviation values, as determined by Neural Net (d_N) and HOSE (d_A) methods (Fig. 4), respectively, was identified as the most probable structure for **1** [28]. Finally, rings B and C were constructed, and the planar structure of **1** with an unprecedented 2,3,7,8,9,9a-hexahydro-4H-furo[3,2-c]chromen-4-one ring system was elucidated as shown in Fig. 4.

The NOESY correlations (Fig. 3) revealed that protons H-3 and H_2-26 were on the same side of the molecule and were assigned a β-orientation. Additionally, the disappearance of the cross-peaks of H-7/H_2-26 implied that H-7 might be adopted in an α-orientation. When only one set of experimental data is available, the DP4$^+$ probability has demonstrated clear superiority over the regression analysis of the NMR data in discriminating isomers [29]. To further confirm the relative configuration of H-7, the DP4$^+$ probability of the two tentative isomers of **1** were calculated using functional B3LYP, with results that confirmed the α-orientation of H-7 (Fig. 5). Furthermore, the absolute configuration of **1** was established by ECD calculation. As depicted in Fig. 6, the calculated ECD curve of (3*S*, 5*R*, 7*S*)-**1** matched the experimental ECD curve, providing evidence for the absolute configuration of **1** as 3*S*, 5*R*, 7*S*.

Hypsampsonione B (**2**) was isolated as a yellow oil and subjected to various spectral analyses to determine its structure. HR-ESI-MS revealed a molecular ion at *m/z* 607.4345 $[M + H]^+$ (Calcd. for $C_{39}H_{59}O_5$: 607.4357), indicating a molecular formula of $C_{39}H_{58}O_5$, with eleven degrees of unsaturation. The ^{1}H NMR spectrum (Tab. 1) revealed the characteristic signals of four olefinic protons (δ_H 5.08, 1H, t, J = 7.2 Hz; 5.02, 1H, t, J = 7.2 Hz; 4.95, 1H, t, J = 7.3 Hz; 4.86, 1H, t, J = 7.3 Hz) and twelve methyl groups (δ_H 2.13, s; 1.70, s; 1.68, s; 1.64, s; 1.60, s; 1.60, s; 1.60, s; 1.58, s; 1.23, d, J = 7.0 Hz; 1.18, d, J = 7.0 Hz; 1.09, s; 1.07, s). Interpretation of the ^{13}C NMR data suggested the presence of four carbonyl groups (δ_C 211.5; 206.3; 205.8; 168.5). Five doubles bonds and four carbonyl groups accorded for 9 degrees of unsaturation. Thus, we speculated that a dicyclic moiety was present in **2** due to the remaining two degrees of unsaturation.

The two-ring system of compound **2** was determined through 2D NMR data analysis. Five distinctive fragments (**a**–**e**) were observed from cross-peaks in the ^{1}H-^{1}H COSY spectrum (Fig. 7). The connections of C-38, C-1, and C-3 to C-2 were established through HMBC correlations from *gem*-dimethyls (Me-38 and Me-39) to C-1, C-2, and C-3. In addition, the HMBC correlative signals from H_2-4 to C-5, C-6, C-15, and C-19, and from H_2-29 to C-7, C-8, C-9, and C-34 indicated the linkages of C-6, C-4, and C-19 *via* C-5, and the

Table 1 ^{1}H (600 MHz) and ^{13}C (150 MHz) NMR data of 1 and 2

No.	1[a]		2[b]	
	δ_H (*J* in Hz)	δ_C	δ_H (*J* in Hz)	δ_C
1		128.2		134.2
2		37.9		38.0
3	1.85 m	40.4	1.52 m	41.5
4a	1.93 overlap	28.9	2.03 overlap	29.9
4b	1.66 overlap		1.50 overlap	
5		40.6		49.6
6		176.5		143.9
7	4.68 dd (10.3, 8.1)	93.0		168.5
8	2.68 m	27.0		59.6
9		99.5		206.3
10a		160.4	2.15 overlap	27.7
10b			1.63 overlap	
11		147.5	5.02 t (7.2)	122.8
12		196.7		133.2
13		137.4	1.60 s	17.9
14	7.88 d (7.5)	129.3	1.70 s	26.6
15	7.54 t (7.5)	129.3		211.5
16	7.66 t (7.5)	134.1	2.93 m	42.2
17	7.54 t (7.5)	129.3	1.23 d (7.0)	18.4
18	7.88 d (7.5)	129.3	1.18 d (7.0)	18.8
19a	0.96 s	26.2	2.42 dd (14.3, 6.6)	33.4
19b			2.17 dd (14.3, 7.8)	
20	0.99 s	21.9	4.86 t (7.3)	116.8
21a	2.17 dd (12.4, 3.7)	27.8		139.9
21b	1.68 overlap			
22	5.16 t (7.1)	123.6	1.99 m	40.2
23		133.0	1.60 s	16.5
24	1.61 s	18.2	2.05 m	26.6
25	1.71 s	28.1	5.08 t (7.2)	123.9
26	2.57 br. d (7.7)	36.7		131.8
27	5.12 t (7.9)	118.4	1.60 s	17.7
28		139.4	1.68 s	25.7
29a	1.93 overlap	40.0	2.62 dd (13.6, 8.5)	32.2
29b			2.51 dd (13.6, 6.6)	
30	1.59 s	16.3	4.95 t (7.3)	118.5
31	2.00 m	26.5		136.3
32	5.08 t (7.5)	124.4	1.58 s	26.0
33		131.3	1.64 s	18.1
34a	1.53 s	18.0	2.01 overlap	31.6
34b			1.92 overlap	
35a	1.62 s	25.9	2.26 dd (10.8, 5.4)	38.1
35b			2.38 dd (10.8, 5.4)	
36		70.6		205.8
37	1.10 s	25.9	2.13 s	29.9
38	1.16 s	25.1	1.07 s	26.0
39			1.09 s	21.6
36-OH	4.75 s			

[a]Measured in DMSO-d_6 [b]Measured in $CDCl_3$

connections of C-29, C-7, C-9, and C-34 to C-8. Further analysis of 1D NMR data revealed a characteristic α, β-unsaturated ketone (δ_C 206.3, 134.2, and 143.9) and a typical ester (δ_C 168.5). The ester carbonyl C-7 and an oxidized olefinic carbon C-6 were connected *via* an oxygen atom, and rings A and B were fused *via* a double bond (C-1 and C-6), which accounted for the last unassigned degree of unsaturation. The presence of two isopentenyl and a geranyl group at C-3, C-8, and C-5, respectively, was deduced from critical HMBC correlations from Me-13 to C-11, C-12, and C-14, from H_2-29 to C-7, C-8, C-9 and C-34, from Me-27 to C-25, C-26 and C-28, from Me-23 to C-20, C-21 and C-22, and from H_2-19 to C-4, C-5, and C-6. Meanwhile, an isobutyryl group attached to C-5 was confirmed by HMBC correlations from Me-17 to C-15 and C-16, and from H_2-4 and H_2-19 to C-15 and C-5. Finally, the presence of a 3-oxobutyl group at C-8 was established through HMBC correlations from Me-37 to C-36 and C-35, and from H_2-34 to C-7, C-8, and C-9. Based on these findings, we proposed a planar structure of compound **2**, as depicted in Fig. 7.

The relative configuration of **2** was assigned using the NOESY experiment (Fig. 7), where the cross-peaks of H-3/Me-38, Me-37/Me-38, and H-16/Me-38 were identified as being β-oriented due to their cofacial relations (Fig. 7). As a result, a 3-oxobutyl and an isobutyryl were assigned to be β-orientation, while two isopentenyls at C-8 and C-3 were assigned as *α*-oritentated. This conclusion was further supported by the NOESY correlations of H-11/Me-28. The absolute configuration of **2** (3*S*, 5*R*, 8*R*) was determined by comparing the experimental ECD with the calculated ECD curves (Fig. 8). Consequently, compound **2** with an unprecedented octahydro-2H-chromen-2-one ring was assigned, as depicted in Fig. 1.

Scheme 1 outlines the hypothetical biosynthetic pathways for two unprecedented seco-PPAPs (**1** and **2**). In Scheme 1A, the plausible biosynthetic pathway of **1** starts with the precursor (**i**), which undergoes isopentenyl transferase and isopentenyl cyclase catalysis to yield intermediate

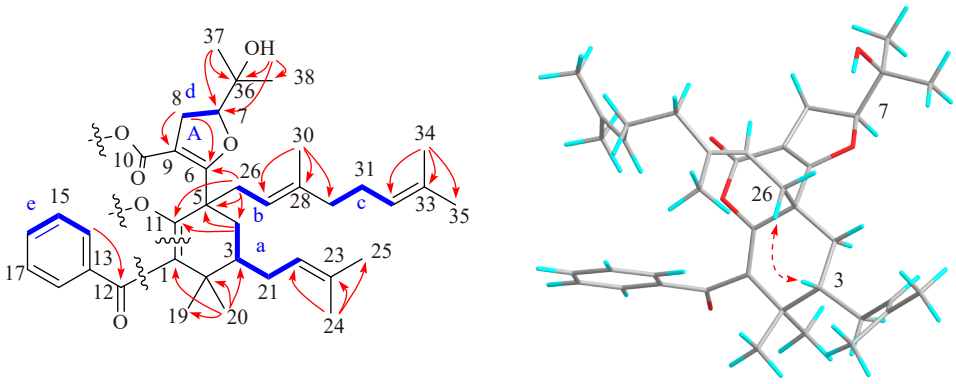

Fig. 3 Key HMBC ⟶, ^{1}H-^{1}H COSY — and NOESY ⇢ correlations of 1.

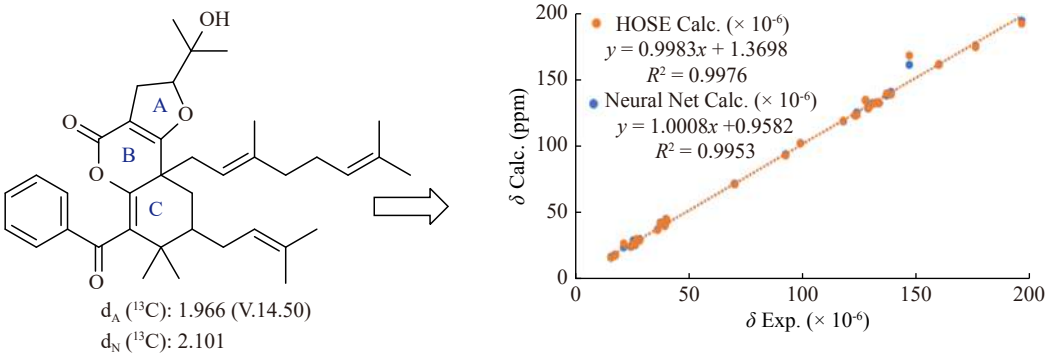

Fig. 4 Top structure generated by Struc. Eluc. software and its linear regression plots through both HOSE and Neural Net methods of ^{13}C chemical shift prediction.

iii. Subsequently, a sequence of retro-Dieckmann reaction, keto-enol tautomerism, and esterification [30] leads to the formation of the key intermediate **vi**, featuring two rare ring systems. Finally, oxidation of a double bond and cyclization processes result in the formation of compound **1**. In Scheme 1B, the plausible biosynthetic pathway of **2** involves a series of isopentenyl transferase, retro-Dieckmann reaction, and isopentenyl cyclase catalysis of 3-isobutyryl phloroglucinol (**i**) to form a vital seco-phloroglucinol derivative (**iv**). Then keto-enol tautomerism and esterification yield intermediate **vi**, followed by migration of a double bond and oxidation, resulting in the formation of compound **2**.

The inhibitory effects of the isolated compounds (**1**–**14**) against *α*-glucosidase were evaluated through *in vitro* assays (Fig. 9). Among the tested compounds, six (**1**, **5**–**8**, and **14**) exhibited significant inhibitory effects, with inhibitory ratios exceeding 50%. To further explore their potential, these compounds were subjected to IC_{50} determination, resulting in a range of IC_{50} values from 0.050 ± 0.0016 μg·mL^{-1} to 366.70 ± 1.08 μg·mL^{-1} (Tab. 2). Notably, compound **5** displayed exceptional *α*-glucosidase inhibitory activity, with an IC_{50} value of 0.050 ± 0.0016 μg·mL^{-1}, surpassing the positive control acarbose by approximately 6900-fold (IC_{50} = 346.63 ± 15.65 μg·mL^{-1}). Interestingly, compounds **3**, **4**, and **5** shared the same xanthone skeleton, but only **5** displayed remarkable inhibitory effects. This observation suggested that the presence of hydroxyl groups at C-3, C-6, and C-7 could obviously enhance the inhibitory activity against *α*-glucosidase. Furthermore, the flavonoid derivatives (**6** and **7**) displayed divergent inhibitory profiles, potentially due to the presence of olefinic bonds between C-2 and C-3 in **7** (IC_{50} = 1.76 ± 0.18 μg·mL^{-1}), contributing to its superior inhibitory effect compared with that of **6** (IC_{50} = 60.72 ± 0.35 μg·mL^{-1}).

In addition, the inhibitory potential of all the isolated compounds against another two key enzymes related to DM, namely PTP1B [31] and α-amylase [32], was also evaluated, and the results are presented in Table. 2. Among the tested compounds, only compound **7** exhibited a slight inhibitory effect against PTP1B, with an IC_{50} value of 85.05 ± 0.71 μg·mL^{-1}. Meanwhile, compound **12** showed a moderate inhibitory effect against α-amylase, with an IC_{50} value of 87.95 ± 3.71 μg·mL^{-1}, compared with that of the positive control acarbose (IC_{50} = 22.47 ± 1.36 μg·mL^{-1}).

Molecular docking is a valuable tool for predicting molecular interactions between a protein and a ligand in the bound state [33]. To investigate the potential molecular interactions between α-glucosidase and α-glucosidase with inhibitory compounds, a novel PPAP (**1**) and the most active xanthone (**5**) were selected for molecular docking studies [34]. As shown in Fig. 10 and Table. 3, both compounds were well-docked into the catalytic site cavity of α-glucosidase. Compound **1** was packed into the catalytic pocket formed by seven amino acid residues of the protein, namely PHE-571, VAL-576, PHE-38, ASN-37, ASP-34, PHE-307, and TRP-528,

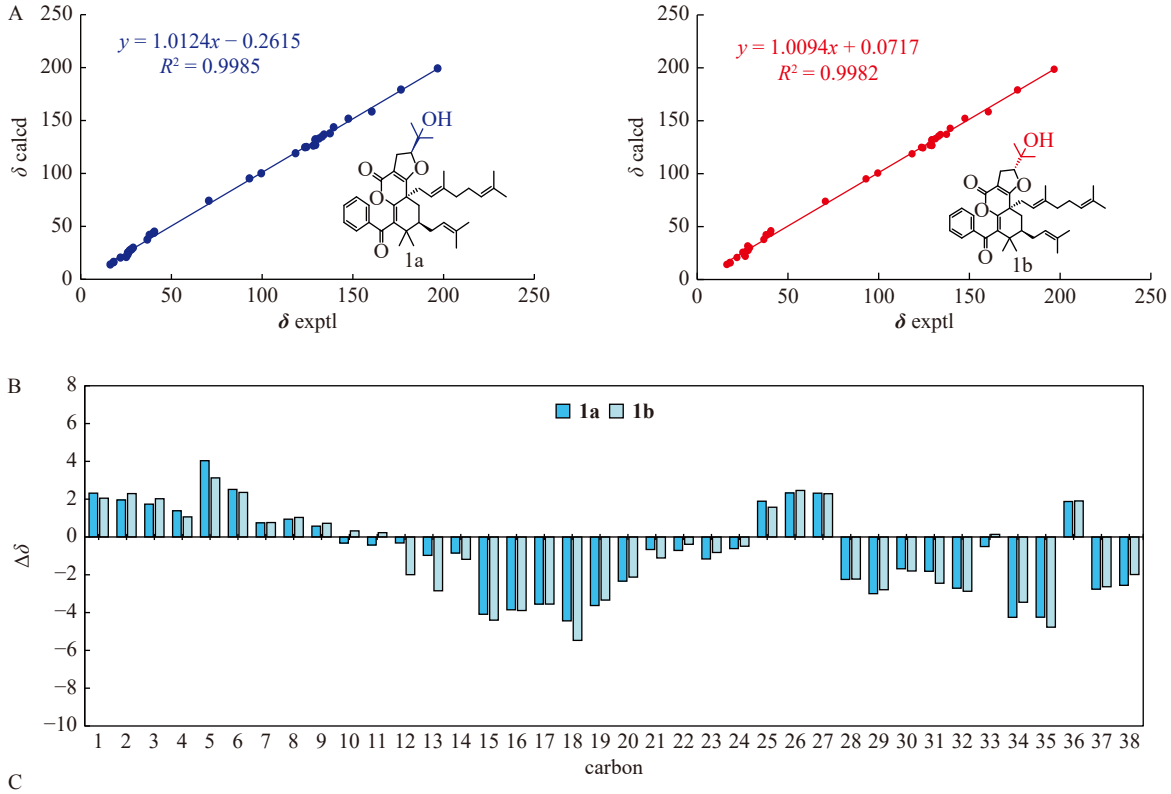

C

	DP4 probability of ^{13}NMR of 1	
Plausible compounds	**1a**	**1b**
Product of probabilities	1.36×10^{-32}	2.16×10^{-33}
Bayes's theorem probability (%)	86	14

Fig. 5 ^{13}C NMR calculation results of two compounds (1a and 1b) at the B3LYP/6-31 + G (d, p) level. (A) Relative errors between the calculated and recorded ^{13}C values. (B) DP4^{+} probability of ^{13}C values of 1.

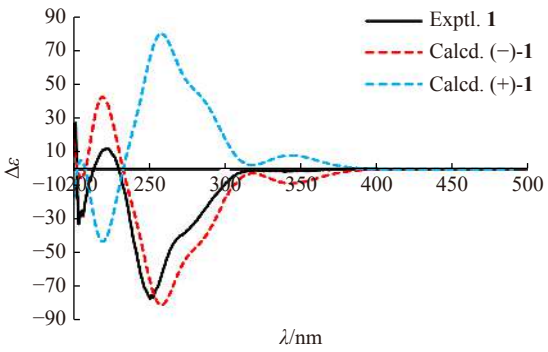

Fig. 6 Experimental and calculated ECD spectra of 1.

with a hydrogen bond formed between compound **1** and ASN-37 (Fig. 10A). Similarly, compound **5** was buried in a hydrophobic pocket formed by THR-40, GLU-297, TRP-344, PRO-314, ARG-300, ARG-35, and LYS-39, with three H-bonds formed between compound **5** and the α-glucosidase (PDB ID: 7K9N) (Fig. 10B). These molecular interactions contributed to the potent inhibitory effect of compound **5** against *α*-glucosidase.

Experimental

Plant collection

The leaves and twigs of *H. sampsonii* were collected from Ziyun County, Guizhou Province, China. The botanical identification was conducted by Mr. Jun Zhang, and a voucher specimen (No. 20191108) was deposited in Natural Products Research Center of Guizhou Province.

Spectroscopic techniques and chromatography

In this study, various spectroscopic techniques were employed to characterize the isolated compounds. ^{1}H, ^{13}C nuclear magnetic resonance (NMR), and 2D NMR spectra were acquired on a Bruker Advance NEO 600 spectrometer using TMS as an internal standard. High-resolution electrospray ionization mass spectrometry (HR-ESI-MS) and ESI-MS were performed on an Agilent 1100 instrument and Thermo ultimate 3000/Q EXACTIVE FOCUS mass spectrometers, respectively. Optical rotations were measured on a JASCOP-1020 polarimeter. UV spectra were detected on a Shimadzu UV-2401PC spectrometer, while IR spectra were obtained on a Bruker FT-IR Tensor-27 and iCAN 9 infrared spectrophoto-

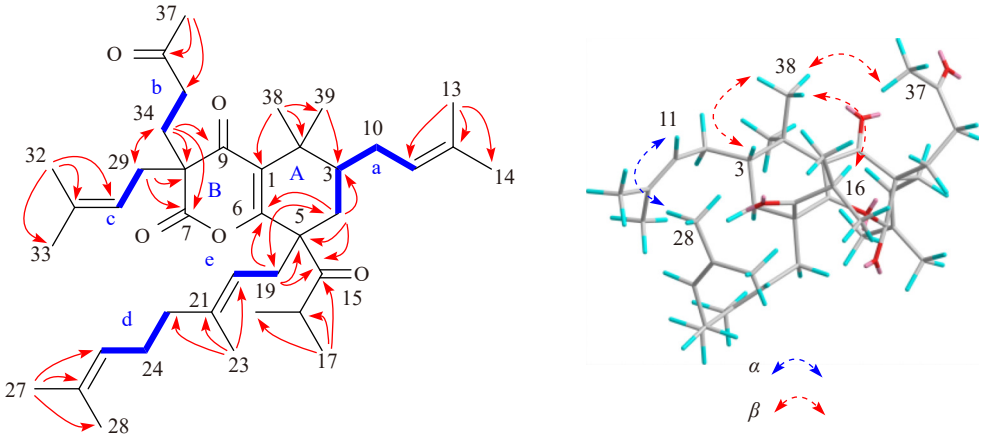

Fig. 7 Key HMBC ⟶, ^{1}H-^{1}H COSY —, and NOESY ⟷ correlations of 2.

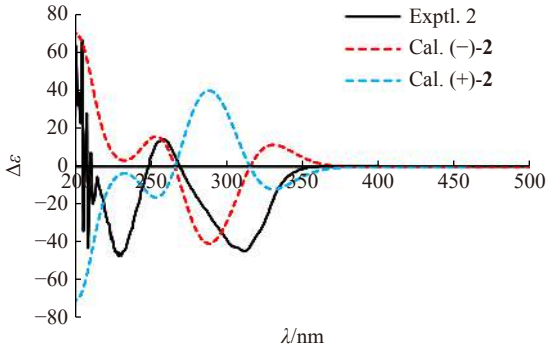

Fig. 8 Experimental and calculated ECD spectra of 2.

meter with KBr disks. Column chromatography was performed on silica gel (300–400 mesh; Qingdao Marine Chemical Co., Ltd., China), RP-C_{18} gel (40–63 μm, Merck, Darmstadt, Germany), and Sephadex LH-20 (40–70 μm, Amersham Pharmacia Biotech AB, Uppsala, Sweden). Semi-preparative HPLC was conducted on an instrument equipped with a Hanbon NP7005c controller, a Hanbon NP7005 pump, and a Hanbon NU3000c dual λ absorbance detector with YMC-Triart-C_{18} column (250 mm × 10.0 mm, 5 μm) and X-bridge-C_{18} column (250 mm × 10.0 mm, 5 μm). Fractions were monitored by TLC (GF 254, Qingdao Marine Chemical Co., Ltd.).

Extraction, isolation, and purification

The air-dried leaves and twigs of *H. sampsonii* (30 kg) were extracted with 150 L MeOH at room temperature three times (five days per time), and the MeOH extracts were combined and evaporated under reduced pressure to give a crude residue (3.3 kg). The crude residue was subjected to a silica gel column chromatography, eluted with petroleum ether-EtOAc (from 100 : 1 to 1 : 100, *V/V*) to obtain ten fractions (Fr. 1–Fr. 10). Fr.2 (210 g) was further divided into 10 subfractions (Fr. 2A–Fr. 2J) over an RP-C_{18} column, eluted with MeOH-H_2O (50 : 50→0 : 100, *V/V*). Subsequent chromatography of Fr. 2A (597 mg) over a silica gel column (petroleum ether-acetone, 80 : 20, *V/V*) and a Sephadex LH-20 column (MeOH) led to the isolation of compounds **3** (10 mg), **9** (18 mg), and **10** (34 mg). Fr. 2C (4.8 g) was separated on a Sephadex LH-20 column (MeOH) to provide three subfractions (Fr. 2Ca–Fr. 2Cc). Fr. 2Ca (57 mg) was purified by semi-preparative HPLC separation (MeOH−H_2O, 94 : 6, *V/V*, 2.0 mL·min^{-1}) to obtain compound **2** (4 mg, t_R = 39.4 min). Compound **13** (38 mg) was obtained from Fr. 2Cc (1.2 mg) through silica gel column chromatography (petroleum ether-EtOAc, 90 : 10, *V/V*). Fr. 2F (200 mg) was fractionated by a silica gel column and further recrystallized from MeOH to yield compound **12** (8 mg). Fr. 3 (110 g) was applied to an RP-C_{18} column washed with MeOH−H_2O (40 : 60→0 : 100, *V/V*) to get nine subfractions (Fr. 3A–Fr. 3I). Fr. 3A (5.99 g) was further purified by a silica gel column eluted with petroleum ether-acetone (9 : 1→1 : 9, *V/V*) to produce compound **8** (14 mg). Compound **14** (9 mg) was isolated from Fr. 3H (2.8g) after repeated silica gel column chromatography. Fr. 5 (40 g) was separated by a RP-18 column eluted with a gradient of MeOH−H_2O (50 : 50→0 : 100, *V/V*) to obtain 11 subtractions (Fr. 5A-Fr. 5K). Fr. 5C (218 mg) was subjected to Sephadex LH-20 (MeOH) to obtain compounds **4** (40 mg) and **1** (10.0 mg). Fr. 7 (81.8 g) was separated by an MCI column eluted with MeOH−H_2O (50 : 50→0 : 100, *V/V*) to get five subfractions (Fr. 7A–Fr. 7E). Fr. 7A (900 mg) was subjected to repeated silica gel column chromatography ($CHCl_3$−EtOAc, 90 : 10, *V/V*) and Sephadex LH-20 column chromatography (MeOH) to isolate compounds **5** (22 mg), **7** (43 mg), and **6** (37 mg).

Chemical characterization

Hypsampsonione A (1): The compound was obtained as a colorless oil with a specific rotation of $[\alpha]_D^{20}$ -164.71 (*c* 3.4, MeOH). Its UV spectrum in MeOH showed absorption maxima (λ_{max}) at 201 nm (log ε 3.88) and 250 nm (log ε 3.42), and its IR spectrum (KBr) exhibited characteristic peaks (ν_{max}) at 2925, 1740, 1666, 1448, 1397, 1225, 1174, 1067, 1045, 923, 892, 850, 740, 688 cm^{-1}.The ^{1}H and ^{13}C NMR data are presented in Tab. 1, and the compound showed a positive HR-ESI-MS peak at *m/z* 587.3728 $[M + H]^+$(Calcd. for $C_{38}H_{51}O_5$, 587.3731).

Hypsampsonione B (2): The compound was obtained as a light yellow oil with a specific rotation of $[\alpha]_D^{20}$ -76.38 (*c*

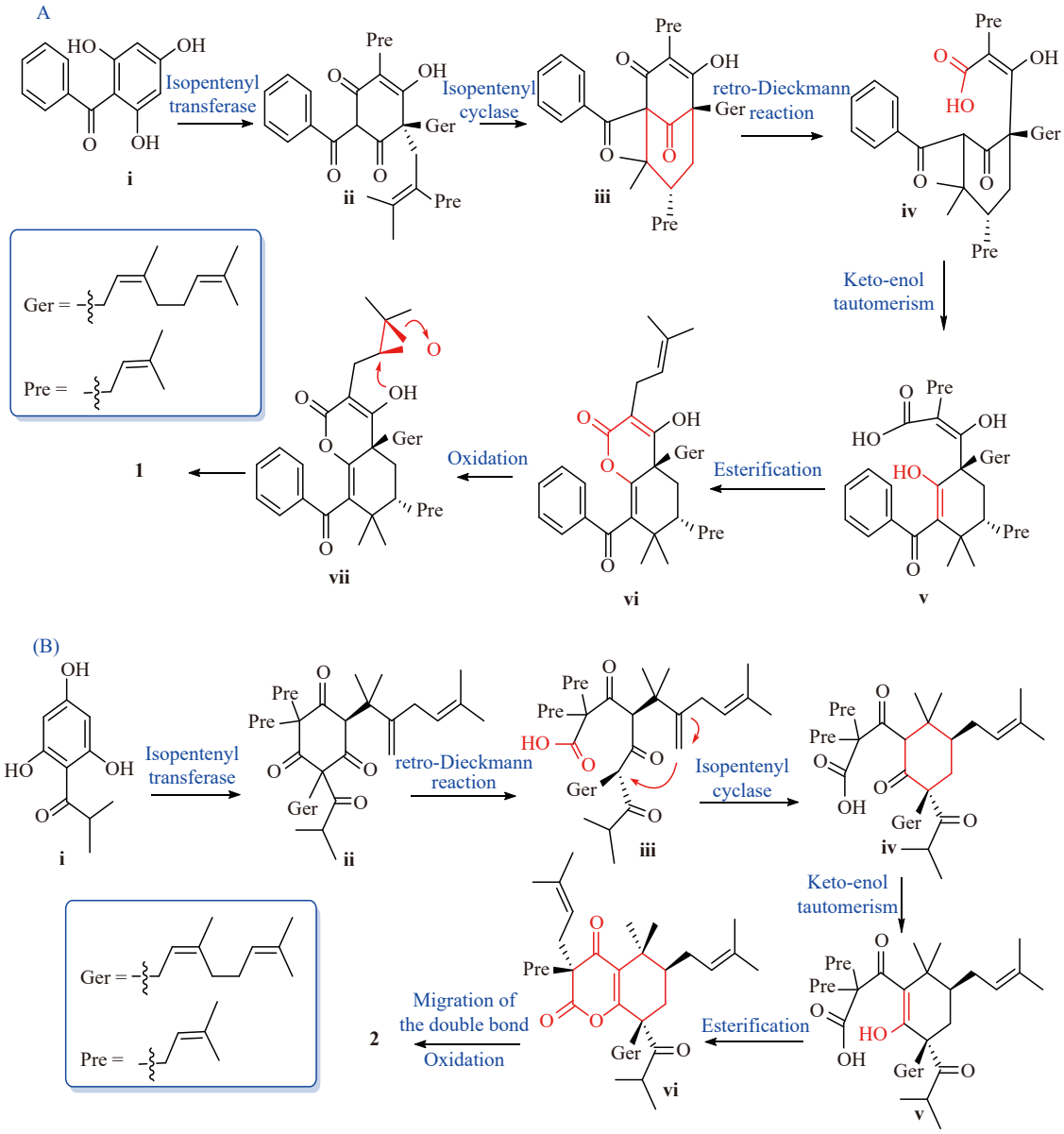

Scheme 1 Hypothetical biosynthetic pathways of 1 and 2. (A) Plausible biosynthetic pathway of 1. (B) Plausible biosynthetic pathway of 2.

1.6, MeOH). Its UV spectrum in MeOH showed an absorption maximum (λ_{max}) at 200 nm (log ε 4.68), and its IR spectrum (KBr) exhibited characteristic peaks (ν_{max}) at 1716, 1685, 1652, 1419, 1380, 1261, 1089, 803 cm^{-1}. The ^{1}H and ^{13}C NMR data are presented in Tab. 1, and the compound displayed a positive HR-ESI-MS peak at *m/z*: $[M + H]^+$ 607.4345 (Calcd. for $C_{39}H_{59}O_5$, 607.4357).

Theoretical ECD calculation

This study employed CONFLEX search to obtain a set of stable conformers for compound **1** and **2** [35]. Subsequently, conformers with a Boltzmann-population exceeding 1% were further optimized through the density functional theory (DFT) method at the B3LYP/6-311 + g (d) level in the Gaussian 09 program package. The equivalent circulating density (ECD) of the conformer of selected conformers was then calculated by the time-dependent DFT (TD-DFT) method at the CAM-B3LYP/tzvp level with the PCM model in methanol solution. Finally, the resulting calculated ECD curve was generated using SpecDis 1.604 [35].

In vitro α-glucosidase inhibitory assay

The inhibitory activity against α-glucosidase (Sigma Aldrich) was evaluated using a modified version of a previously reported procedure [36]. Briefly, 70 μL of PBS buffer (10 mmol·L^{-1}), 10 μL of the test samples (500 μg·mL^{-1} as the initial concentration), and 20 μL of the enzyme (0.5 U·mL^{-1} in PBS) were sequentially added into 96-well plates, followed by incubation of the samples at 37 °C for 15 min. Next, 20 μL of the substrate p-nitrophenyl α-D-glucopyranoside (0.25 mmol·L^{-1}) was added, and the enzymatic reaction was performed at 37 °C for 30 min, followed by the addition

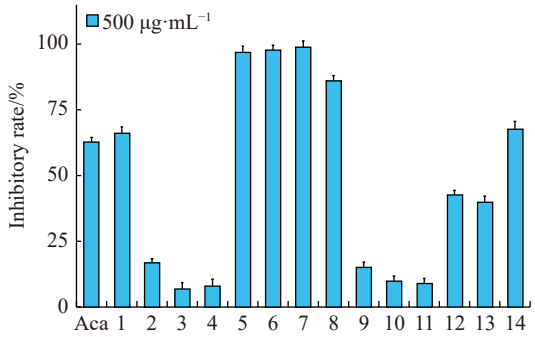

Fig. 9 α-Glucosidase inhibitory rate for isolates. Aca: the positive control, acarbose.

Table 2 Inhibitory activities of compounds 1, 5–8, 12, and 14 against α-glucosidase, α-amylase, and PTP1B with IC_{50} values (μg·mL^{-1}).

Comp.	IC_{50} (μg·mL^{-1}) [a,c]		
	α-Glucosidase	α-Amylase	PTP1B
1	317.10 ± 1.27	> 200	> 200
5	0.050 ± 0.0016	> 200	> 200
6	60.72 ± 0.35	> 200	> 200
7	1.76 ± 0.18	> 200	85.05 ± 0.71
8	94.10 ± 1.03	> 200	> 200
12	> 500	87.95 ± 3.71	> 200
14	366.70 ± 11.08	> 200	> 200
Acarbose[b]	346.63 ± 15.65	22.47 ± 1.36	-[d]
Suramin[b]	-[d]	-[d]	46.71 ± 2.17

[a] IC_{50}: half maximum inhibitory concentration.

[b] Acarbose and suramin were used as positive controls for those three enzymes.

[c] Compounds **2**–**4**, **9**–**11**, and **13** were inactive for those three enzymes.

[d] -: not test.

of 80 μL of Na_2CO_3 (80 mmol·L^{-1}) to stop this reaction. Finally, the absorbance of the solvent was measured at 405 nm. The positive control, acarbose, was adopted for comparison.

In vitro protein tyrosine phosphatase 1B inhibitory assay

The PTP1B enzyme (Sino Biological Inc., Beijing, China) [31] was used to evaluate the inhibitory activity of the compounds. A modified version of the previously reported method [31] was employed for the screening assay. In short, a working buffer comprising of MOPS (34.5 mmol·L^{-1}), DTT (2 mmol·L^{-1}), EDTA (0.69 mmol·L^{-1}), BSA (2 mg·mL^{-1}), and NaCl (2 mol·L^{-1}) was prepared for the assay. 70 μL of working buffer, 10 μL of PTP1B enzyme (5 μg·mL^{-1} in working buffer), and 10 μL of tested samples (dissolved in DMSO) were added in sequence into 96-well plates and pre-incubated at 37 °C for 15 min. The enzymatic reaction was initiated by adding 10 μL of substrate p-NPP (100 mmol·L^{-1} in working buffer). After incubation at 37 °C for 30 min, the reaction was terminated by addition of 0.1 mol·L^{-1} Na_2CO_3. The absorbance of the reaction mixture was measured at 405 nm using a microplate reader (Thermo Varioskan LUX, Waltham, USA). Suramin was used as the positive control.

In vitro α-amylase inhibitory assay

The inhibitory activity against α-amylase (Sigma Aldrich) was determined using a previouslly reported method with minor modifications [32]. Briefly, different concentrations of each sample (25 μL) and 10 μL of α-amylase solution (5 U·mL^{-1}) were pre-incubated in PBS at 37 °C for 10 min. After pre-incubation, the reaction was initiated by adding 100 μL of starch solution (0.5% in water heated at 100 ºC for 15 min) and tempered at 37 ºC for another 10 min. Then the reaction was terminated by adding 25 μL of 0.1 mol·L^{-1} HCl. Iodine-potassium iodide solution (KI/I_2 3 : 1, 50 μL) was added to each well to measure the absorbance of the samples. Finally, the absorbance was read at 630 nm after the plate was incubated at 37 °C for 12 min. The blank of each concentration was prepared by adding all reaction reagents without α-amylase enzyme solution. In the negative control and the positive control, solvent alone and solvent with acarbose were used to replace samples respectively, following the same protocol used for tested samples.

Molecular docking

Molecular docking analysis of compounds **1** and **7** with α-glucosidase was performed using AutoDock software, following the method described in previous studies [33][34]. The α-glucosidase protein (PDB ID: 7K9N) was retrieved from the Protein Data Bank. Hydrogen atoms were added, and the crystallographic water molecules in 7K9N were removed. At neutral pH, all the dissociable residues in the system were set as default. For further docking, the edited 7K9N and ligand files were transcribed into PDBQT format files, and all the parameters were set as default.

Conclusion

In the present study, we employed a bioactivity-guided isolation approach to investigate the chemical constituents of *H. sampsonii*. This led to the isolation of two highly modified seco-PPAPs (**1** and **2**) and twelve known ones (**3**–**14**). Notably, compounds **1** and **2** featured an unprecedented octahydro-2H-chromen-2-one ring system. Among the isolated compounds, six (**1**, **5**–**7**, **9**, and **14**) exhibited promising inhibitory effects against α-glucosidase. In particular, compound **5** displayed the most potential inhibitory activity against α-glucosidase, which was about 6900 times more potent than the positive control. Furthermore, a molecular docking study was conducted to gain insight into molecular interactions between two compounds (**1** and **5**) and α-glucosidase. To the best of our knowledge, this is the first report on the anti-diabetic effect of *H. sampsonii*, providing new insights into the therapeutic potential of this traditional Chinese medicine.

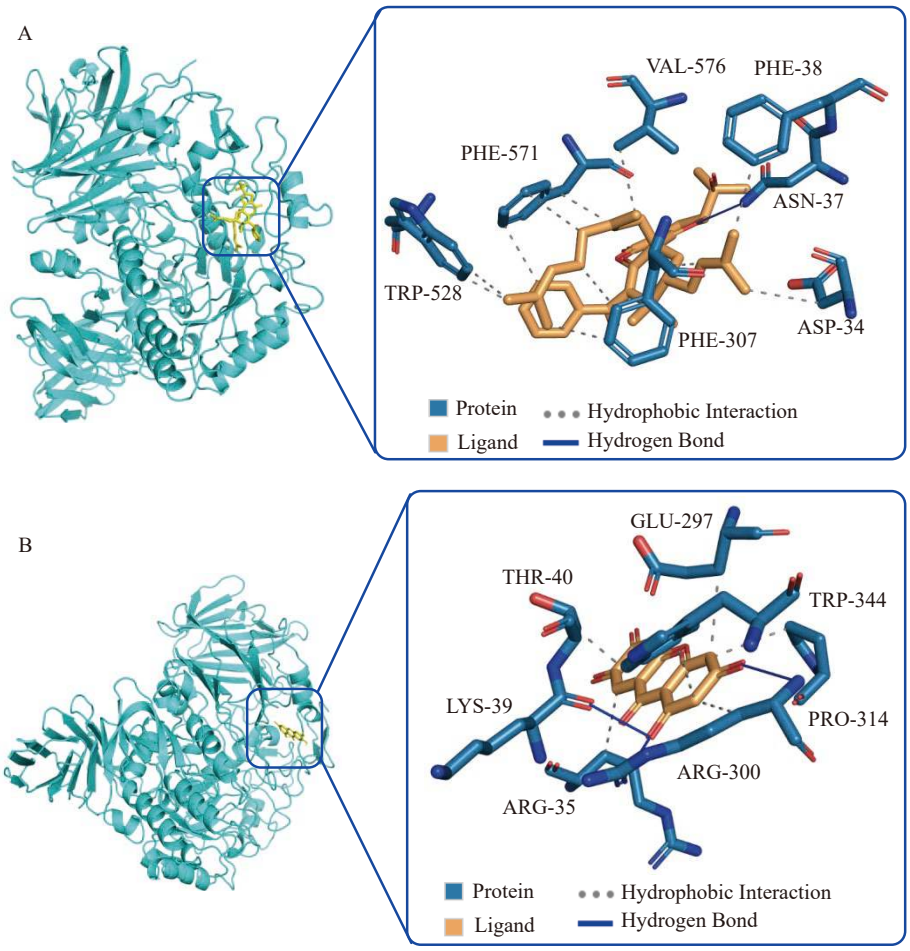

Fig. 10 Docking studies of compounds 1 and 5 with α-glucosidase (pdb: 7K9N). (A) Binding pose of compound 1 with α-glucosidase. (B) Binding pose of compound 5 with α-glucosidase.

Table 3 Interaction information of compounds 1 and 5 with α-glucosidase

Comp.	Interaction amino acids	Hydrogen bonds
1	PHE-571, VAL-576, PHE-38, ASN-37, ASP-34, PHE-307, TRP-528	ASN-37
5	THR-40, GLU-297, TRP-344, PRO-314, ARG-300, ARG-35, LYS-39	LYS-39, ARG-35, PRO-314

Appendix A. Supplementary data

Supplementary data to this article can be abtained by E-mail to corresponding author.

References

[1] Maliwal D, Pissurlenkar RRS, Telvekar V. Identification of novel potential anti-diabetic candidates targeting human pancreatic α -amylase and human α -glycosidase: an exhaustive structure-based screening [J]. *Can J Chem*, 2022, **100**(5): 338-352.

[2] Ashraf J, Mughal EU, Sadiq A, *et al*. Design and synthesis of new flavonols as dual *a*-amylase and *a*-glucosidase inhibitors: structure-activity relationship, drug-likeness, *in vitro* and *in silico* studies [J]. *J Mol Struct*, 2020, **1218**: 128458.

[3] Yilmazer-Musa M, Griffith AM, Michels AJ, *et al*. Grape seed and tea extracts and catechin 3-gallates are potent inhibitors of α-amylase and α-glucosidase activity [J]. *J Agric Food Chem*, 2012, **60**(36): 8924-8929.

[4] Bolen S, Feldman L, Vassy J, *et al*. Systematic review: comparative effectiveness and safety of oral medications for type 2 diabetes mellitus [J]. *Ann Intern Med*, 2007, **147**(6): 386-399.

[5] Bellesia A, Tagliazucchiauthor D. Cocoa brew inhibits *in vitro*-glucosidase activity: the role of polyphenols and high molecular weight compounds [J]. *Food Res Int*, 2015, **63**: 439-445.

[6] Johnson TO, Ermolieff J, Jirousek MR. Protein tyrosine phosphatase 1B inhibitors for diabetes [J]. *Nat Rev Drug Discov*, 2002, **1**(9): 696-709.

[7] Silva AR, Taofiq O, Ferreira ICFR, *et al*. *Hypericum* genus cosmeceutical application–A decade comprehensive review on its multifunctional biological properties [J]. *Ind Crops Prod*, 2021, **159**: 113053.

[8] Hu LH, Sim KY. Sampsoniones A−M, a unique family of caged polyprenylated benzoylphloroglucinol derivatives, from *Hypericum sampsonii* [J]. *Tetrahedron* , 2000, **56** (10): 1379-1386.

[9] Nguyen D, Le V, Nguyen T, *et al*. Bioactive compounds from the aerial parts of *Hypericum sampsonii* [J]. *Nat Prod Res*, 2021, **35**(4): 646-648.

[10] Tian WJ, Yu Y, Yao XJ, *et al*. Norsampsones A−D, four new decarbonyl polycyclic polyprenylated acylphloroglucinols from *Hypericum sampsonii* [J]. *Org Lett*, 2014, **16**(13): 3448-3451.
[11] Zhu H, Chen C, Yang J, *et al*. Bioactive acylphloroglucinols with adamantyl skeleton from *Hypericum sampsonii* [J]. *Org Lett*, 2014, **16**(24): 6322-6325.
[12] Zhang ZZ, Zeng YR, Li YN, *et al*. Two new *seco*-polycyclic polyprenylated acylphloroglucinol from *Hypericum sampsonii* [J]. *Org Biomol Chem*, 2021, **19**(1): 216-219.
[13] Dharmaratne HRW, Napagoda MT, Tennakoon SB. Xanthones from roots of *Calophyllum thwaitesii* and their bioactivity [J]. *Nat Prod Res*, 2009, **23**(6): 539-545.
[14] Fernandes EGR, Silva AMS, Cavaleiro JAS, *et al*. ^{1}H and ^{13}C NMR Spectroscopy of mono - , di - , tri - and tetrasubstituted xanthones [J]. *Magn Reson Chem*, 1998, **36**(4): 305-309.
[15] Hong SS, Suh HJ, Oh JS. Phenolic chemical constituents of the stem barks of *Robinia pseudoacacia* [J]. *Chem Nat Compd*, 2017, **53**(2): 359-361.
[16] Agrawal PK, Agarwal SK, Rastogi RP, *et al*. Dihydroflavanonols from *Cedrus deodara*, A ^{13}C NMR study [J]. *Planta Med*, 1981, **43**(9): 82-85.
[17] Adfa M, Yoshimura T, Komura K, *et al*. Anti-termite activities of coumarin derivatives and scopoletin from *Protium javanicum* Burm. f. [J]. *J Chem Ecol*, 2010, **36**(7): 720-726.
[18] Henry GE, Campbell MS, Zelinsky AA, *et al*. Bioactive acylphloroglucinols from *Hypericum densiflorum* [J]. *Phytother Res*, 2009, **23**(12): 1759-1762.
[19] Bakker BH, Steinberg H, de Boer TJ. The chemistry of small ring compounds. Part 35. Oxidation of arylcyclopropanone methyl hemiacetals by cupric ions and by oxygen [J]. *Recl Trav Chim Pays-Bas*, 1976, **95**(11): 274-277.
[20] Zhang JS, Huang JL, Zou YH, *et al*. Novel degraded polycyclic polyprenylated acylphloroglucinol and new polyprenylated benzophenone from *Hypericum sampsonii* [J]. *Phytochem Lett*, 2017, **21**: 190-193.
[21] Zhao X, Guo Y, Xu Q, *et al*. (±)-Hyperpyran A: terpenoid-based bicyclic dihydropyran enantiomers with hypoglycemic activity from *Hypericum perforatum* (St. John's wort) [J]. *Fitoterapia*, 2022, **161**: 105221.
[22] Cichewicz RH, Kouzi SA. Chemistry, biological activity, and chemotherapeutic potential of betulinic acid for the prevention and treatment of cancer and HIV infection [J]. *Med Res Rev*, 2004, **24**(1): 90-114.
[23] Chiang YM, Kuo YH. Two novel α-tocopheroids from the aerial roots of *Ficus macrocarpa* [J]. *Tetrahedron Lett*, 2003, **44**(27): 5125-5128.
[24] Kim KH, Lee KH, Choi SU, *et al*. Terpene and phenolic constituents of *Lactuca indica* L [J]. *Arch Pharm Res*, 2008, **31**(8): 983-988.
[25] Xu WJ, Zhu MD, Wang XB, *et al*. Hypermongones A−J, rare methylated polycyclic polyprenylated acylphloroglucinols from the flowers of *Hypericum monogynum* [J]. *J Nat Prod*, 2015, **78**(5): 1093-1100.
[26] Elyashberg M, Argyropoulos D. Computer assisted structure elucidation (CASE): current and future perspectives [J]. *Magn Reson Chem*, 2021, **59**(7): 669-690.
[27] Bai M, Zhao WY, Zhang YJ, *et al*. The identification of alkaloids from the stems of *Picrasma quassioides via* computer-assisted structure elucidation and quantum chemical calculations [J]. *J Asian Nat Prod*, 2021, **23**(3): 217-227.
[28] Lv TM, Guo R, Yan ZY, *et al*. Structure elucidation of a new terpenylated coumarin with the combination of CASE algorithms and DFT/NMR approach [J]. *J Asian Nat Prod Res*, 2021, **23**(10): 982-991.
[29] Tang Y, Zhao ZZ, Hu K, *et al*. Irpexolidal represents a class of triterpenoid from the fruiting bodies of the medicinal fungus *Irpex lacteus* [J]. *J Org Chem*, 2019, **84**(4): 1845-1852.
[30] Huang L, Zhang ZZ, Li YN, *et al*. Hypersampones A−C, three nor-polycyclic polyprenylated acylphloroglucinols with Lipid-Lowering activity from *Hypericum sampsonii* [J]. *Org Lett*, 2022, **24**(32): 5967-5971.
[31] Tahtah Y, Wubshet SG, Kongstad KT, *et al*. High-resolution PTP1B inhibition profiling combined with high-performance liquid chromatography-high-resolution mass spectrometry-solid-phase extraction-nuclear magnetic resonance spectroscopy: proof-of-concept and antidiabetic constituents in crude extract of *Eremophila lucida* [J]. *Fitoterapia*, 2016, **110**: 52-58.
[32] Faraone I, Russo D, Genovese S, *et al*. Screening of *in vitro* and *in silico* α-amylase, α -glucosidase, and lipase inhibitory activity of oxyprenylated natural compounds and semisynthetic derivatives [J]. *Phytochemistry*, 2021, **187**: 112781.
[33] Meng XY, Zhang HX, Mezei M, *et al*. Molecular docking: a powerful approach for structure-based drug discovery [J]. *Curr Comput Aided Drug*, 2011, **7**(2): 146-157.
[34] Karade SS, Hill ML, Kiappes JL, *et al*. *N*-substituted valiolamine derivatives as potent inhibitors of endoplasmic reticulum α-glucosidases I and II with antiviral activity [J]. *J Med Chem*, 2021, **64**(24): 18010-18024.
[35] Li YN, Zeng YR, Yang J, *et al*. Chemical constituents from the flowers of *Hypericum monogynum* L. with COX-2 inhibitory activity [J]. *Phytochemistry*, 2022, **193**: 112970.
[36] Chen Z, Hao J, Wang L, *et al*. New α -glucosidase inhibitors from marine algae-derived Streptomyces sp. OUCMDZ-3434 [J]. *Sci Rep*, 2016, **6**(1): 1-9.

Cite this article as: TAO Linlan, XU Shuangyu, ZHANG Zizhen, LI Yanan, YANG Jue, GU Wei, YI Ping, HAO Xiaojiang, YUAN Chunmao. Bioassay-guided isolation of α-Glucosidase inhibitory constituents from *Hypericum sampsonii* [J]. *Chin J Nat Med*, 2023, **21**(6): 443-453.